Evapotranspiration and Soil Moisture Dynamics in a Temperate Grassland Ecosystem in Inner Mongolia, China

L. Hao, G. Sun, Y.-Q. Liu, G. S. Zhou, J. H. Wan,
L. B. Zhang, J. L. Niu, Y. H Sang, J. J. He

Abstract. *Precipitation, evapotranspiration (ET), and soil moisture are the key controls for the productivity and functioning of temperate grassland ecosystems in Inner Mongolia, northern China. Quantifying the soil moisture dynamics and water balances in the grasslands is essential to sustainable grassland management under global climate change. We conducted a case study on the variability and characteristics of soil moisture dynamics from 1991 to 2012 by combining field monitoring and computer simulation using a physically based model, MIKE SHE, at the field scale. Our long-term monitoring data indicated that soil moisture dramatically decreased at 50, 70, and 100 cm depths while showing no obvious trend in two other layers (0-10 cm and 10-20 cm). The MIKE SHE model simulations matched well to measured daily ET during 2011-2012 (correlation coefficient R = 0.87; Nash-Sutcliffe NS = 0.73) and captured the seasonal dynamics of soil moisture at five soil layers (R = 0.36-0.75; NS = 0.06-0.42). The simulated long-term (1991-2012) mean annual ET was 272 mm, nearly equal to the mean precipitation of 274 mm, and the annual precipitation met ET demand for only half of the years during 1991 to 2012. Recent droughts and lack of heavy rainfall events in the past decade caused the decreasing trend of soil moisture in the deep soil layers (50-100 cm). Our results show that precipitation dominated the water balances in the grassland, and the balance between ET and precipitation explained the seasonal changes of soil water content in different soil layers. We conclude that the persistent drought and change in precipitation patterns of decreasing large storm events as well as total rainfall were the main causes for the observed drying trend in soils in the 2000s, although we could not exclude other impacts from regional hydrologic alterations, such as groundwater overdraft.*

Keywords. *Climate change, Evapotranspiration, MIKE SHE model, Soil moisture, Water balance.*

Soil moisture is a major component of the hydrologic cycle that is highly variable and nonlinear in space and time (Heathman et al., 2012), controlling the interactions between the land surface and atmospheric process (Brubaker and Entekhabi, 1996). Soil moisture plays a critical role in how an ecosystem responds to the physical environment through its influence on the surface energy budget and the partitioning of rainfall into runoff or infiltration (Joshi et al., 2011). This is especially true in arid and semi-arid temperate grasslands where water availability is a major limiting factor for ecosystem functions (Zhang and Liu, 2014). In the past decades, global climate change and human activity have profoundly impacted terrestrial ecosystems (Chanasyk et al., 2003), especially grassland ecosystems (Fay et al., 2003). Climate change and human disturbances due to overgrazing, mining, and water overuse can change rangeland ecosystems considerably through altering the land use/cover patterns and ecosystem water balances (Sun et al., 2008; Hao et al., 2014, 2015). Characterizing the spatiotemporal dynamics of soil moisture across multiple scales is essential in environmental applications of remote sensing technology, as well as for hydrologic modeling (e.g., model validation) (Heathman et al., 2012; Han et al., 2012; Starks et al., 2003). Soil moisture exhibits high spatial-temporal variability over multiple scales. Knowledge of the patterns of soil moisture in arid environments is important for protecting and restoring vegetation, optimizing agricultural production, and managing soil and water resources. However, long-term soil moisture data are rare in China due to the difficulty of sampling in arid environments (Zhang and Shao, 2013).

Submitted for review in December 2014 as manuscript number NRES 11099; approved for publication by the Natural Resources & Environmental Systems Community of ASABE in July 2015.

Mention of company or trade names is for description only and does not imply endorsement by the USDA. The USDA is an equal opportunity provider and employer.

The authors are **Lu Hao,** Professor, International Center for Ecology, Meteorology, and Environment (IceMe), Jiangsu Key Laboratory of Agricultural Meteorology, Nanjing University of Information Science and Technology, Nanjing, China; **Ge Sun,** Research Hydrologist, Eastern Forest Environmental Threat Assessment Center, USDA Forest Service Southern Research Station, Raleigh, North Carolina; **Yongqiang Liu,** Research Meteorologist, Center for Forest Disturbance Science, USDA Forest Service Southern Research Station, Athens, Georgia; **Guangsheng Zhou,** Professor, Institute of Botany, Chinese Academy of Sciences, Beijing, China; **Jinhong Wan,** Research Hydrologist, China Institute of Water Resources and Hydropower Research, Beijing, China; **Libo Zhang,** Graduate Student, **Jianlong Niu,** Graduate Student, and **Yihui Sang,** Graduate Student, IceMe, Jiangsu Key Laboratory of Agricultural Meteorology, Nanjing University of Information Science and Technology, Nanjing, China; **Junjie He,** Senior Engineer, Xilinhot National Climatological Observatory, Xilinhot, Inner Mongolia, China. **Corresponding author:** Ge Sun, USDA Forest Service Southern Research Station, 920 Main Campus Dr., Venture Center 2, Suite 300, Raleigh, NC 27606; phone: 919-515-9498; e-mail: gesun@fs.fed.us.

A number of field studies have detected the temporal changes in soil moisture in arid and semi-arid environments dominated by various ecosystems (Brocca et al., 2007; Grassini et al., 2010; Sala et al., 1992; Wendroth et al., 1999). Zhang and Liu (2014) simulated water fluxes during the growing season in the Xilin River basin using the Grassland Landscape Productivity Model (GLPM). Their results demonstrated that water fluxes varied in response to spatiotemporal variations in environmental factors and associated changes in plant phenological and physiological characteristics. Li et al. (2011) examined the spatial and temporal variations in soil moisture in China using a regional climate model, CLM3.5, and found that the arid and semi-arid region had the highest soil moisture variations during the past five decades.

To a large extent, soil water resources depend on soil depth in addition to local climate (Jia and Shao, 2014). However, current agronomic, hydrological, pedological, and environmental studies have tended to focus on soil water in the shallow layers (Tombul, 2007; Famiglietti et al.; 1998; Wang et al., 2013). Soil water in deeper layers has largely been ignored due to the high measurement cost in labor and time required (Jia and Shao, 2014; Mohanty et al., 1998). Developing accurate water balances at the watershed to regional scale requires a detailed understanding of the soil moisture storage change in the entire soil profile. Impacts of groundwater withdrawals on soil moisture in different layers are rarely studied. Therefore, there has been a great interest in studying soil moisture in deep layers in a variety of ecosystems in arid regions to better understand the interactions among soil water dynamics, climate, and vegetation restoration and management (Yang et al., 2014; Sun et al., 2005).

The Xilin Gol grassland is one of the few well-preserved areas of the Inner Mongolia grassland region in northern China (Hao et al., 2014). This region has uneven distributions of both water and heat, and thus large variations in primary productivity (Shao et al., 2013) and hydrologic regimes (Zhou and Wang, 2002). During the past three decades, the grassland ecosystem in Xilin Gol has been seriously deteriorating under the combined effects of climate change, land use change, and socioeconomic transformation (Liu et al. 2013; Qi et al., 2012; Hao et al., 2014). Conservation efforts in this region have focused on restoring the ecological functions in reducing wind erosion and dust storms in a changing climate (Qi et al., 2012; Hao et al., 2014). Detecting the trends and variability in soil moisture and their interconnections with surface hydrological processes such as precipitation and ET patterns in the region offers insights to the observed environmental changes (i.e., land degradation, groundwater decline, and climate change).

Using the Xilin Gol grassland as one example, this study aimed at understanding the observed soil moisture dynamics using field monitoring and long-term water balance simulation with a validated computer model (MIKE SHE). The specific objectives of this study were to explore the following questions: (1) Has the soil moisture changed significantly during the past 22 years (1991-2012) in a typical grassland on the Inner Mongolia Plateau? (2) Could climate change and variability explain the observed changes in soil moisture? (3) Could simulated long-term ET and water balances explain the observed soil moisture dynamics? and (4) Could the changes of measured grass biomass productivity be explained by changes in ET and soil moisture at the study site? Our central hypothesis was that deeper soil moisture content (>50 cm) is controlled by the long-term climatic change and variability and by the balances between precipitation and ET.

Materials and Methods

Long-term soil moisture dynamics have been routinely monitored at selected national standard climate stations as one of the parameters to provide information on meteorological and water stress conditions throughout China. In this study, we selected one of these sites in Xilin Gol, Inner Mongolia, as a case study (fig. 1). We examined the relationships between soil moisture content and climate at the field scale by analyzing accumulated soil moisture and ET time series data and developing soil water balances. The analysis was assisted by a computer simulation model (MIKE SHE) that was parameterized and validated with ET measured by the lysimeter method and soil moisture measurements (fig. 2). The MIKE SHE model has been widely used in semi-arid and humid regions in China and the U.S. to understand the effects of climate and land use change on hydrological balances at the watershed scale (Tague et al., 2004; McMichael et al., 2006; Sun et al., 2006; Zhang et al., 2008; Lu et al., 2009; Dai et al., 2010).

Location and Climate

The Xilin Gol grassland (41° to 47° N, 111° to 120° E) is located in the central part of the Eurasian Steppe (fig. 1). This region represents the typical temperate steppe ecosystem, which forms the major native grasslands of Inner Mongolia in China. The terrain is characterized by low hills, and the slope is moderate (fig. 1). The vegetation at the grassland research site is dominated by *Stipa krylovii* and *Leymus chinensis* communities. The soil is dominated by chestnut soil (Chinese soil taxonomy). The climate is characterized as a continental temperate arid climate with four distinctive seasons, long and cold winters, and short frost-free periods. The annual mean precipitation is 278 mm, occurring mainly in June to August with a large intra-annual variability (fig. 3). Annual snowfall is about 17 mm, or 6% of total precipitation, occurring mainly from November to March. The potential ET as estimated by the FAO reference ET method exceeds precipitation in this region, resulting in an arid climate (fig. 3). The annual average temperature is 2.4°C with large annual and daily temperature fluctuations. Data collected at this research site have been incorporated into the global soil moisture database and have been compared and validated by Robock et al. (2000). Regionally, groundwater depths showed a significant declining trend of 5 cm per year during January 2006 to August 2010 at two observation sites in West Ujimqin Banner and Abag Banner in the Xilin Gol grassland region, 100 to 150 km from our soil moisture study

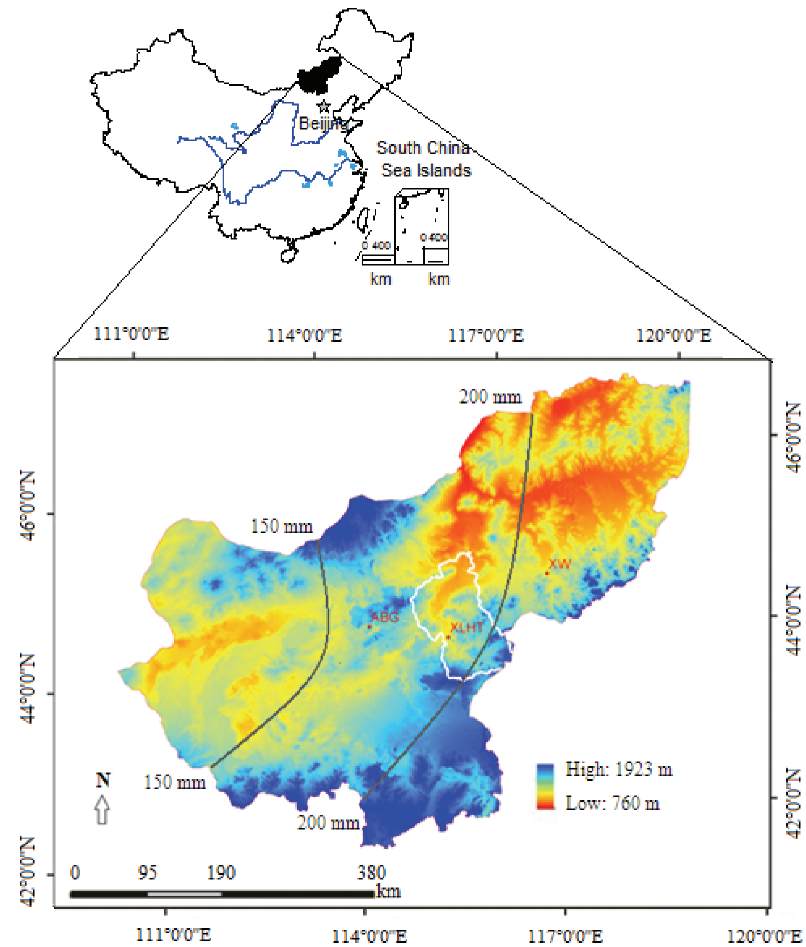

Figure 1. Research site location, precipitation distribution, and topography in the Xilin Gol League in Inner Mongolia, northern China. The lines are total precipitation during April-August. XW = West Ujimqin Banner, ABG = Abag Banner, and XLHT = Xilinhot, where the Xilinhot National Climatological Observatory is located.

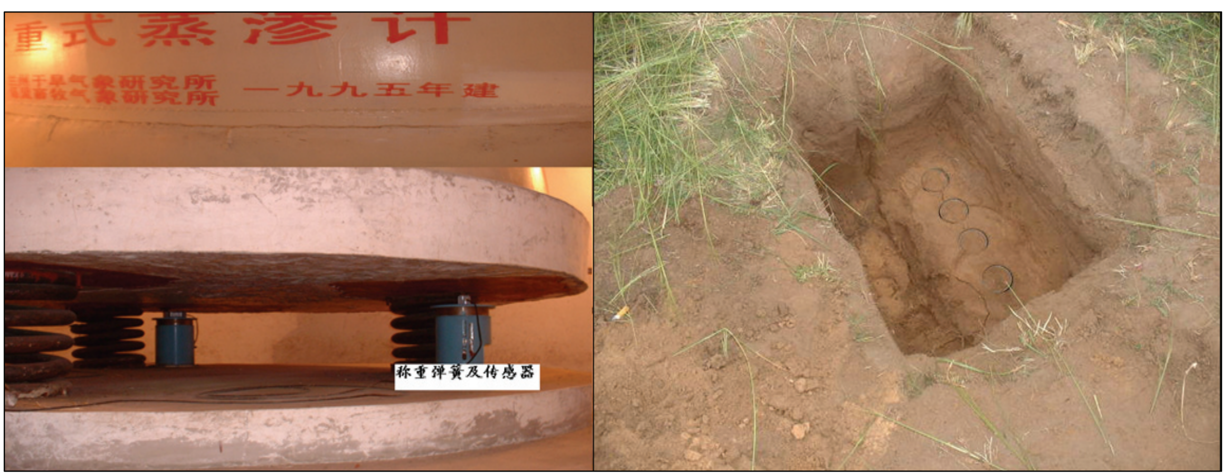

Figure 2. Photos showing the weighing lysimeter and soil moisture sampling profiles at the Xilinhot National Climatological Observatory.

site (fig. 1). The growing season in this region is from April to September, with the peak growing season from June to August. The soil moisture samples were collected at a research site (XLHT) maintained by the Xilinhot National Climatological Observatory (43° 57′ N, 116° 7′ E) (fig. 1).

In Situ Measurements

Climate, Soil Moisture, and Plant Biomass

The standard meteorological data were collected during 1992-2012 at the Xilinhot National Climatological Observatory, which was operated by the China Meteorological Administration (CMA). Meteorological data including precipitation, radiation, temperature, wind speed, and humidity

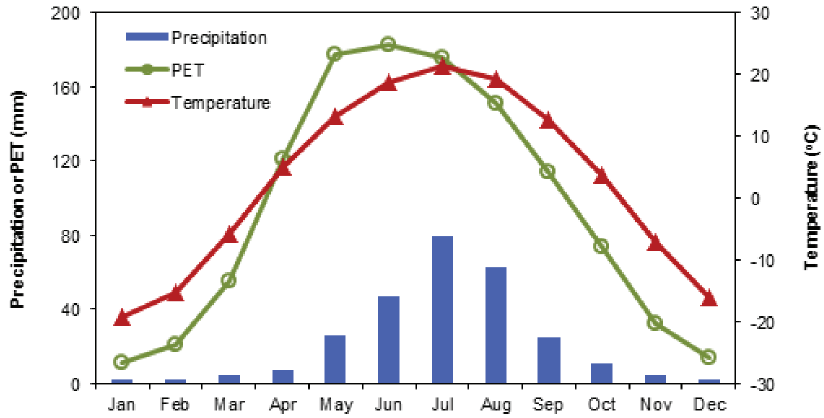

Figure 3. Mean monthly mean climatic variables, precipitation, potential evapotranspiration, and air temperature measured at the Xilin Gol grassland research station on the Mongolia Plateau, northern China (1992-2012).

were used to estimate FAO 56 reference ET (ET_o) as an input to the MIKE SHE hydrological model to develop soil water balances. The aboveground fresh biomass for the native grass covers at the research site was determined around August 25 to 30 of each year during 2004-2011 (Hao et al., 2014).

Soil moistures were manually sampled using the gravimetric method at the Xilinhot National Climatological Observatory (fig. 2) every ten days per month, usually on the 8th, 18th, and 28th. The entire soil moisture monitoring area at the site had four subplots with four replications. During each soil moisture sampling, one replication was conducted in one sub-plot, and the current sampling site was 1 to 2 m away from the previous site. The sampling sites had no disturbance history, i.e., no irrigation or grazing. Soil samples were taken at five soil depths (10, 20, 50, 70, and 100 cm) when soils were not frozen. There were 18 measured data points from April to September in a particular year at each soil depth. The weight-based soil field capacity and the bulk density were measured every five years. The relative soil moisture was estimated with a gravimetric method and expressed as:

$$R_{sm} = \frac{w}{f_c} \times 100\% \qquad (1)$$

where R_{sm} is relative soil moisture, f_c is field capacity (weight based), and w is soil moisture content (weight based), which is calculated as:

$$w = \frac{m_w - m_d}{m_d} \times 100\% \qquad (2)$$

where m_w is wet soil weight, and m_d is dry soil weight. The weight based soil moisture content was changed to the volume based for MIKE SHE model validation purposes.

The Mann-Kendall test (Mann, 1945; Kendall, 1975) was used to test the temporal non-linear trend, and significance levels of $\alpha = 0.01, 0.05$, and 0.1 were applied.

ET Measured by Weighing Lysimeter Method

Daily ET rate for 2011-2012 was estimated by the weighing lysimeter method. The weighing lysimeter quantifies ET directly using a mass balance approach. Therefore, the condensation of gaseous water was ignored when calculating ET, and the data during rainy periods were removed or adjusted. The effective ET area of the lysimeter was 4.0 m^2 with a 2.6 tall, undisturbed soil column (fig. 2). The measurement accuracy of the lysimeter was 0.1 mm. The lysimeter was located about 20 m away from soil moisture sampling site. The data were collected automatically and recorded every hour. Daily ET data were checked for consistency for rainy dates when problems occurred most often. Before the growing season, the weighing method was used to calibrate the lysimeter to ensure data reliability.

MIKE SHE MODEL

The water balances between precipitation input and ET output reflect deep soil water recharge. The seasonal contrasts between precipitation and ET determine the soil moisture dynamics and thus the water available for plant use. We used MIKE SHE to develop long-term site-level water balances after the model was calibrated and verified. MIKE SHE (DHI, 2004) is a physically based hydrological model that simulates the full hydrological cycle at a field or watershed scale (Abbott et al., 1986a, 1986b). In MIKE SHE, ET can be divided into three main components: evaporation from the canopy, transpiration from plants, and evaporation from soils. The three components are based on empirical equations by Kristensen and Jensen (1975). The one-dimensional Richards equation is solved numerically for pressure head variation in the unsaturated zone, which in turn is converted to soil moisture content from the soil moisture retention curve. Groundwater recharge is simulated as well if groundwater is present and interacts with the unsaturated zone. A fixed lateral no-flow boundary was assumed for this flat site for a field-scale simulation study. Essentially, no surface or lateral groundwater flows were allowed in this "point-level" 1-D simulation. The model was parameterized (table 1) to simulate the full site-level water cycle of grasslands at a daily scale and verified with daily ET (2011-2012) measured by a weighing lysimeter, as discussed above. Grass reference ET (ET_o) was calculated following the FAO Penman-Monteith method (Allen et al., 1998) based on daily climatic data. Daily leaf area index (LAI) data were obtained by linear interpolation of the eight-day MODIS LAI dataset that was verified with meas-

Table 1. Key parameters for simulating soil moisture and daily ET in a grassland ecosystem by the MIKE SHE model.

Parameter	Value
Plant rooting depth	250 mm
Daily leaf area index (LAI)	Variable (0 to 1.8)
Potential evapotranspiration (PET)	Variable (0 to 12 mm d^{-1})
Initial groundwater table depth	-6 m
Soil hydraulic conductivity	50 (shallow layers) to 7.7 (deep layers) × 10^{-5} m s^{-1}
Coefficient of canopy interception	0.05 mm
C1, C2, and C3 (ET parameters)	0.2, 0.3, and 20

Table 2. Estimated parameters for the van Genuchten equation describing the soil water retention curves at different soil depth.

Soil Layer	θ_r	θ_s	α	n
0-10 cm	0.0157	0.2514	0.0899	1.3627
10-20 cm	0.0047	0.1615	0.0500	1.3839
20-30 cm	0.0186	0.1147	0.0335	1.8938
40-50 cm	0.0133	0.1094	0.0437	1.9369

ured monthly LAI during from 2004 to 2006 (May to September). The soil textures and root depths at the research sites were obtained from field soil samples. The van Genuchten parameters (θ_s, θ_r, n, α) for the water retention curves of the soils were estimated by least square curve fitting of the van Genuchten function to the measured relationships between soil matric potential (h) and volumetric water content (θ) (Xie et al., 2009). The parameters θ_s and θ_r are the saturated and residual soil water contents, respectively, and n and α control the shape of the h-θ curve (van Genuchten et al., 1998) (table 2). We used correlation coefficient (R), root mean square error (RMSE), and Nash-Sutcliffe model efficiency (NS) to evaluate the performance of the MIKE SHE model in matching daily ET and soil moisture measurements at four different soil depths. In addition, we used relative error (F) to indicate model bias. The 2011-2012 period was used for model calibration against measured soil moisture. The model was not calibrated against ET data.

RESULTS

MEASURED SOIL MOISTURE DYNAMICS

Relative soil moisture in the 10 cm and 20 cm layers showed a general decreasing trend initially in the 1990s, reaching the lowest levels about 2003, and then gradually increasing in the most recent ten years (fig. 4). In contrast, the measured soil moisture at the 50, 70, and 100 cm depths dramatically decreased in the past two decades. The soil moisture at the 100 cm depth had an average value of 53%, similar to the 10 cm layer (51%), during the 1990s, but decreased to 38%, much less than that of the 10 cm layer (46%), in the most recent 12 years. The lowest soil moisture during the two decades was at the 70 cm depth. As expected, the shallow layers, both 10 and 20 cm, fluctuated more than the deep layers (fig. 4).

The M-K test showed that soil moisture content exhibited a significant decreasing trend at 50 and 100 cm, and a highly significant decreasing trend at 70 cm, but a weak decreasing trend at 10 and 20 cm (table 3).

RESPONSE OF SOIL MOISTURE TO ANNUAL RAINFALL AND INDIVIDUAL RAINFALL EVENTS

Annual mean air temperature significantly increased ($p < 0.001$) in the past decades, while precipitation did not show significant change ($p > 0.05$) from 1956 to 2013 as a whole (fig. 5). However, both the total amount and intensity of precipitation decreased during the past two decades (fig. 6). Annual precipitation in the 2000s was 217 mm, much less than that of the 1990s (311 mm). In the growing season, precipitation also obviously decreased from 290 mm in the 1990s to 195 mm in the 2000s (fig. 6a). The total number of days with daily precipitation ≥10 mm in the 2000s was 51 days, which was obviously less than the 81 day in the 1990s, and the total number of days with daily precipitation ≥25 mm in the 2000s (18 days) was also lower than that in the 1990s (7 days) (fig. 6b). This was also true for the growing season. The reductions in total annual and seasonal precipitation and heavy rainfall events shown in figure 6 apparently led to less rainfall infiltrating to the deep soil layers, resulting in drier soils in the deeper soil layers (fig. 6). We further validate this observation in the following sections using individual storm event data and long-term modeled water balances.

The dynamics of soil moisture after four selected storm events with different precipitation illustrate the influence of storm size on infiltration and soil water content at five different depths (fig. 7). When the ten-day accumulated precipitation was about 30 mm, the relative soil moisture at shallow soil layers (0 to 50 cm) increased greatly, and deep layers at 50 to 100 cm had little response (fig. 7). However, after a large 70 mm storm that did not alter soil moisture deeper than 50 cm (July 8, 1999), a small storm of 15 mm could increase the soil moisture at the 50 cm depth (July 18, 1999) (fig. 7c), reflecting the accumulative effects and soil water redistribution within the soil profile. When the ten-day precipitation was 117 mm, soil moisture in both shallow and deeper layers reacted (fig. 7d). The decreases in soil moisture (August 28, 2004) in the deep layer (100 cm) reflected soil drainage, not ET, during August 18-28, 2004.

The short-term soil moisture content in the shallow layers in this arid environment was tightly controlled by precipitation patterns. Storm sizes were critical to soil moisture variations in deep layers that received soil water recharge only when the rainfall amount exceeded certain threshold. These storm-event data indicate that episodic extreme high rainfall events were essential to recharge deeper soil layers in this arid environment.

MODELED ET, SOIL MOISTURE CONTENT, AND WATER BALANCES

Measured soil moisture content (fig. 4) for the 2010-2012 period was used for model calibration (not shown), and the period from 1990 to 2009 was used for model validation (fig. 8). The model was able to capture the high fluctuations of soil moisture in the first layer (10 cm) in response to rainfall events (fig. 8a). For the entire modeling period, a reasonable correlation coefficient of 0.75 was achieved in spite of the low NS = 0.42, RMSE = 0.03, F = 10.9%. For the 50 cm layer, the soil moisture was simulat-

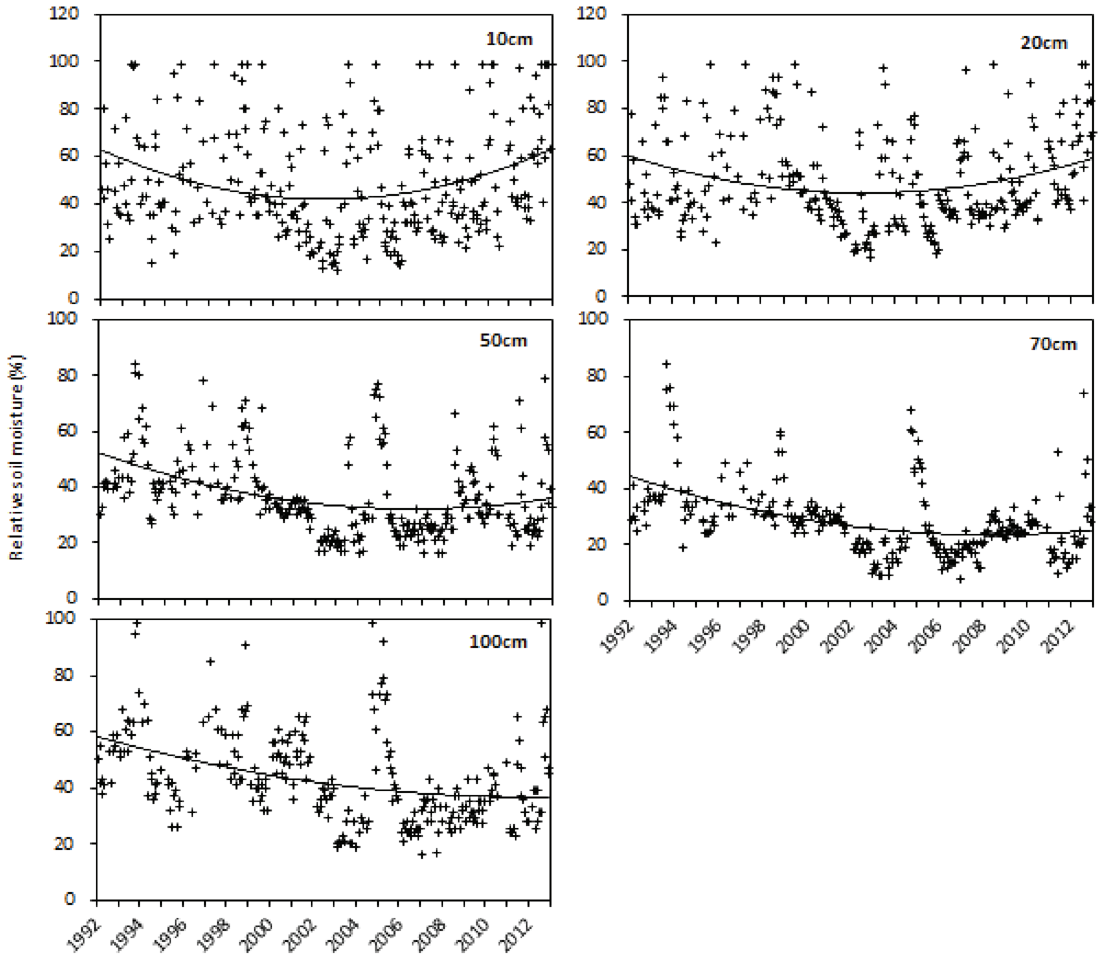

Figure 4. Soil moisture dynamics measured every ten days for different soil layers at 10, 20, 50, 70, and 100 cm depths measured during April-September, 1992-2012, in Xilin Gol grassland, northern China.

ed with R = 0.40, RMSE = 0.04, F = 14.6%, and NS = 0.03 (fig. 8b). For the 70 cm layer, the soil moisture fluctuations were less dramatic as compared to first layer (fig. 8c) and were simulated with R = 0.59, RMSE = 0.03, F = 4.9%, and improved NS = 0.28. The model performed less well for the soil moisture at the 100 cm layer, with R = 0.36, NS = 0.06, RMSE = 0.03, and F = 16.1% (fig. 8d). Overall, the MIKE SHE model performance was unsatisfactory (Ritter and Muñoz-Carpena, 2013) for soil moisture simulation.

The MIKE SHE model was verified with daily ET (2011-2012) measured by a weighing lysimeter and measured soil moisture content at different depths. The model captured daily ET dynamics acceptably (fig. 9), resulting in NS = 0.73, RMSE = 0.62, F = 1.3%, and R = 0.87. Overall, the simulation results indicated that the MIKE SHE model was reliable in evaluating long-term water balances that were controlled by precipitation and ET (fig. 10).

The simulated long-term (1960-2012) mean annual ET was 255 mm, or 93% of the mean precipitation of 275 mm (fig. 10). The remaining 7% became deep seepage to groundwater below the grass rooting zone. The water balance simulation results showed that, during the past 22 years (1990-2012), precipitation met the ET demand in only half of the years. In most years, precipitation was less than the long-term average (fig. 10). Annual ET in the recent decade was low due to the persistent dry climate (fig. 11). This persistent water deficit was likely the reason for the observed decline of soil moisture content in the deep soil layers (>70 cm).

Table 3. Z statistics by nonparametric Mann-Kendall trend tests for soil moisture content at different soil depths (1992-2012).[a]

	Soil Depth				
	10 cm	20 cm	50 cm	70 cm	100 cm
Z statistic	-0.45	-0.48	-2.18*	-2.70**	-1.72^{+}

[a] Symbols indicate significance levels: ** = 0.01, * = 0.05, and $^{+}$ = 0.1.

Interactions among Seasonal ET, Precipitation , and Soil Moisture in Normal, Dry, and Wet Years

Seasonal dynamics of the soil moisture profile were controlled by temporal distributions of precipitation and ET (fig. 12). The year 2010 represents a normal year, receiving 277 mm of precipitation, and the modeled ET (275 mm $year^{-1}$) was barely balanced by precipitation (fig. 12a). The differences in relative soil moisture in the deep soil layers (70 cm) were small, but they were large for the shallow layers (<50 cm). In the dry year of 2011, the annual precipitation was 227 mm, 48 mm less than the long-term av-

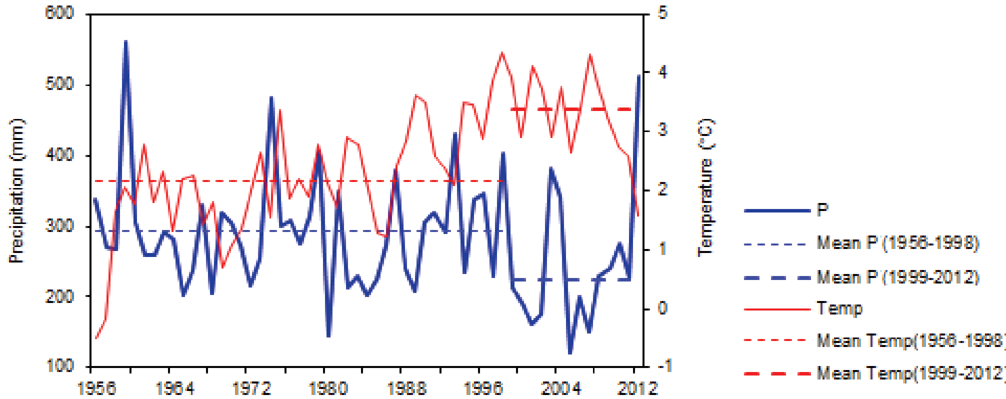

Figure 5. Precipitation (P) and temperature (Temp) change during the period from 1956 to 2013.

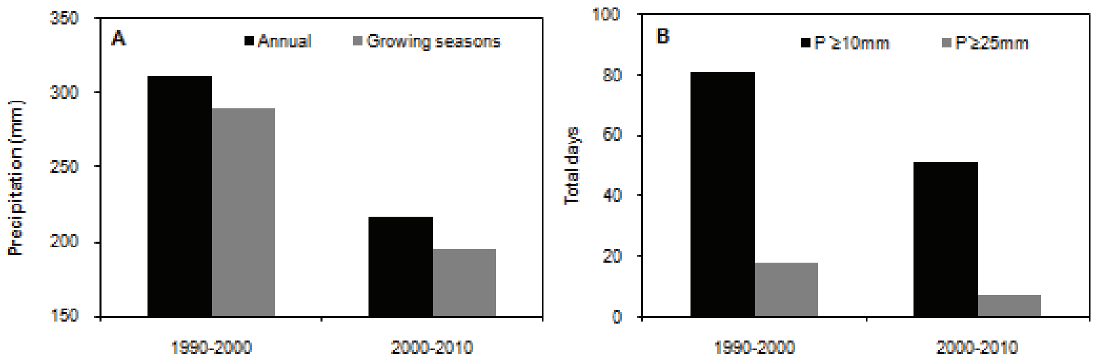

Figure 6. Comparison of (a) annual and growing season precipitation and (b) number of days with daily precipitation (P) ≥ 10 mm or 25 mm during recent two decades.

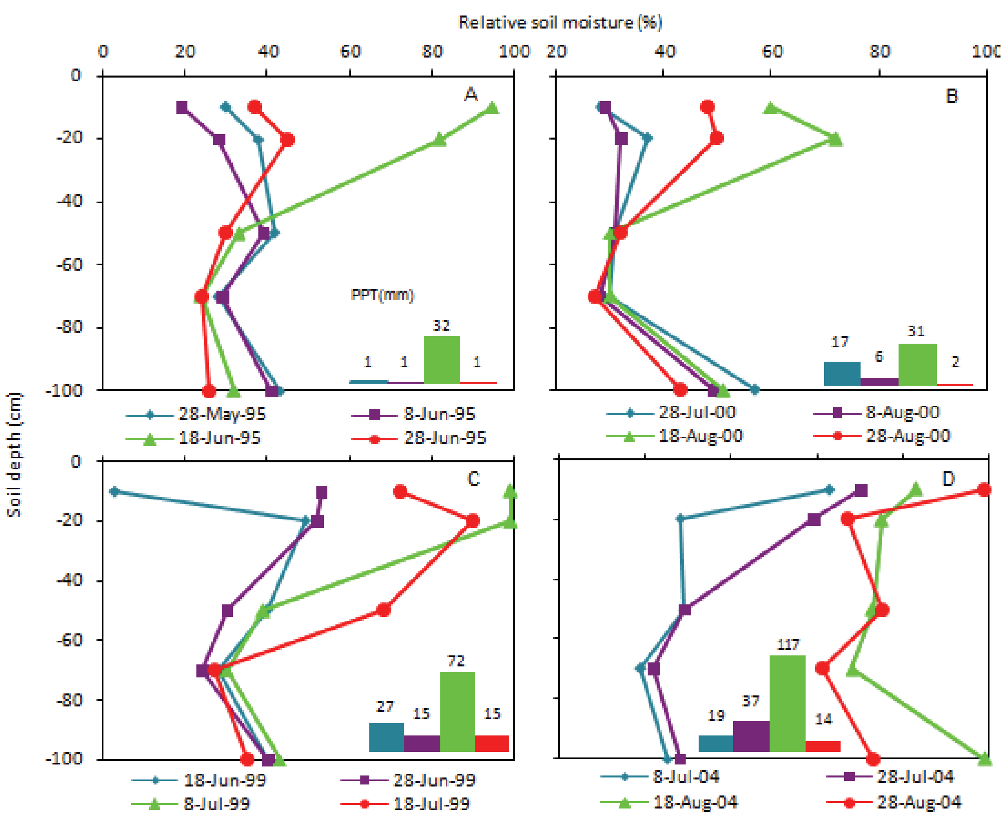

Figure 7. Response of relative soil moisture at five soil layers to accumulated ten-day precipitation. Inset bar charts are total precipitation prior to the soil measurements.

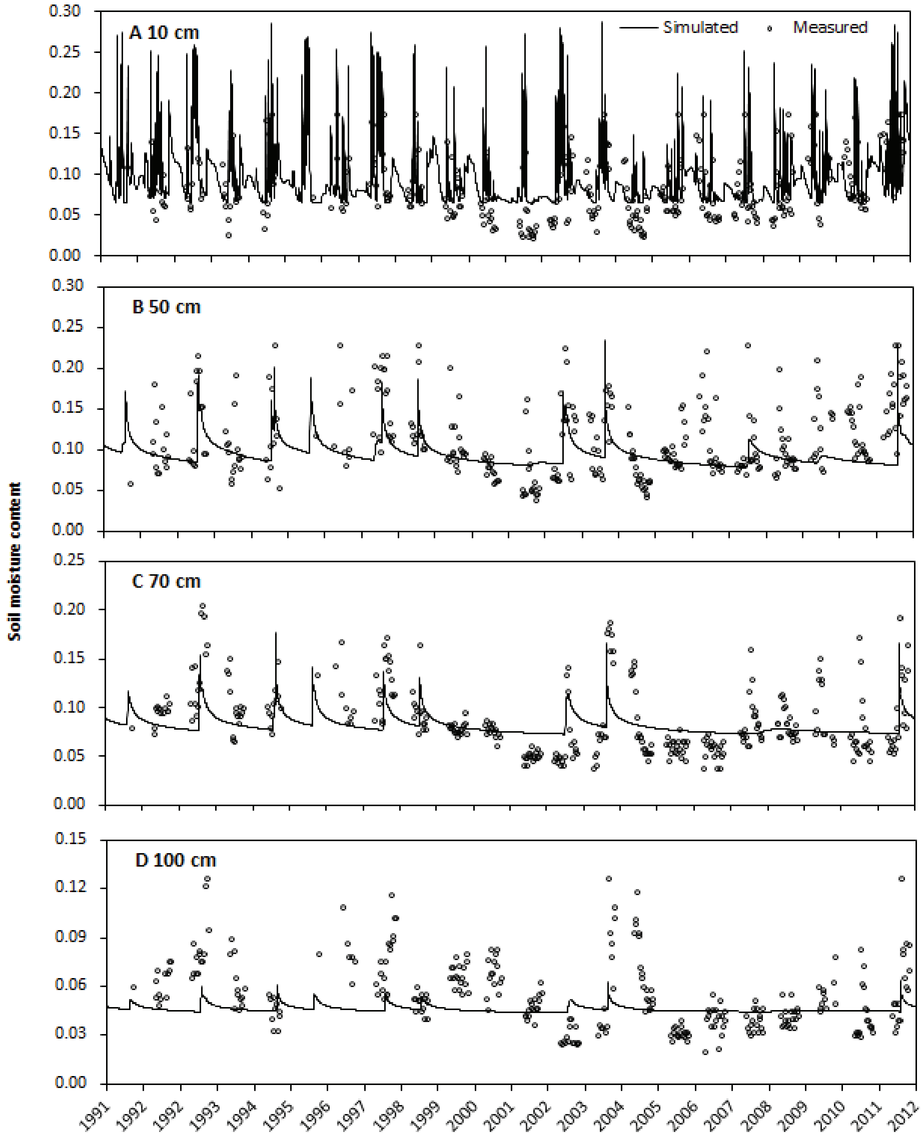

Figure 8. Simulated and measured soil moisture content (volume based) at (a) 10, (b) 50, (c) 70, and (d) 100 cm depths during 1990-2009.

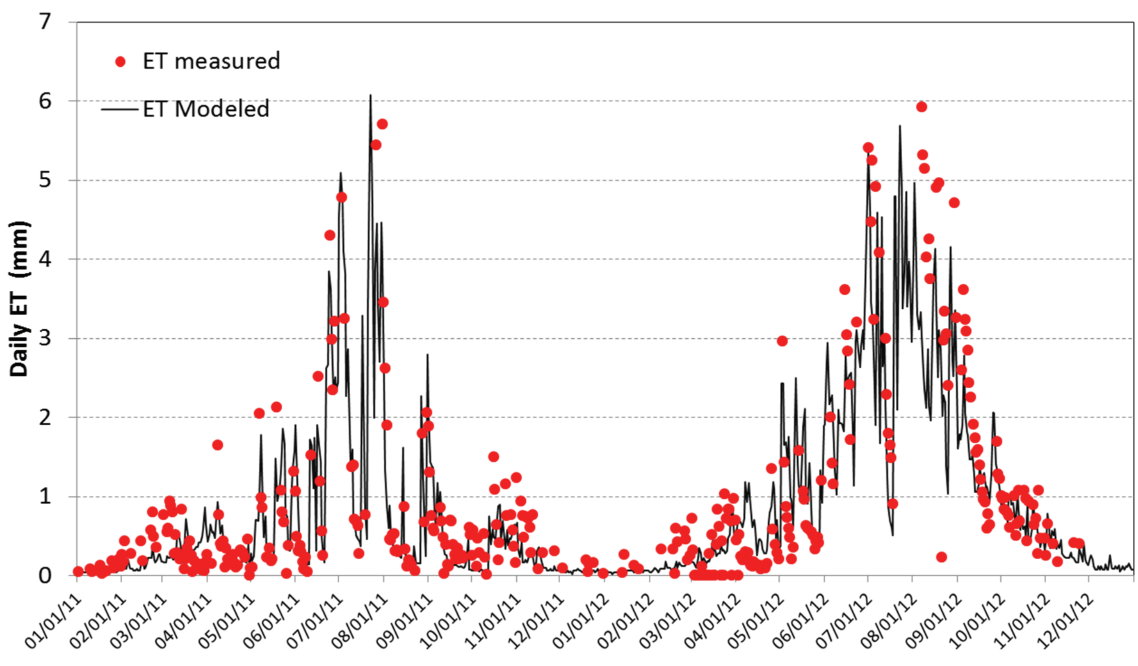

Figure 9. Simulated and measured daily ET of a grassland ecosystem during 2011-2012 in Xilin Gol, Inner Mongolia.

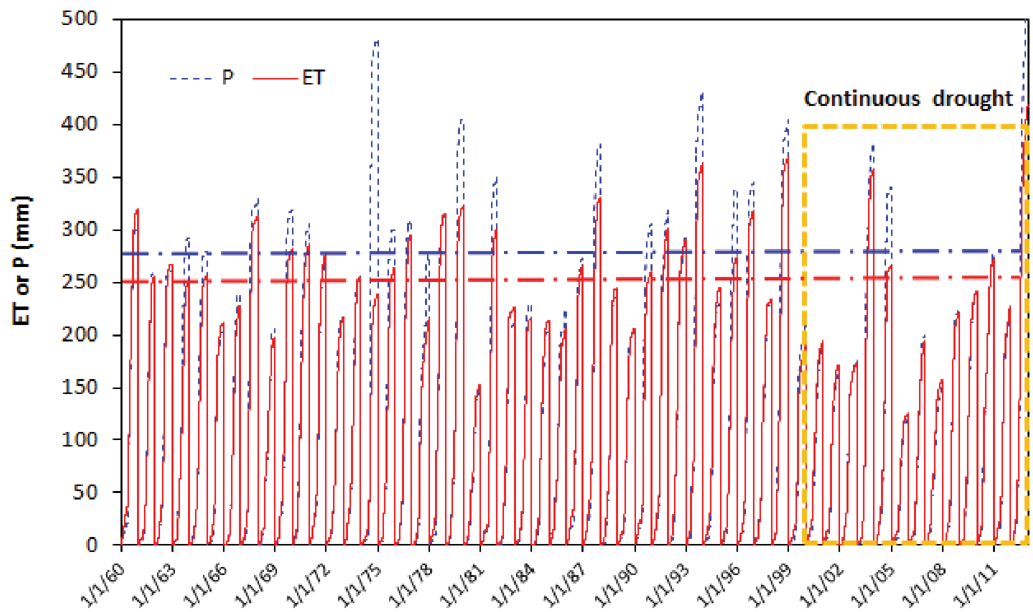

Figure 10. Cumulative precipitation (P) and modeled ET during 1960 to 2012. Dot-dashed lines are long-term mean P (top) and ET (bottom).

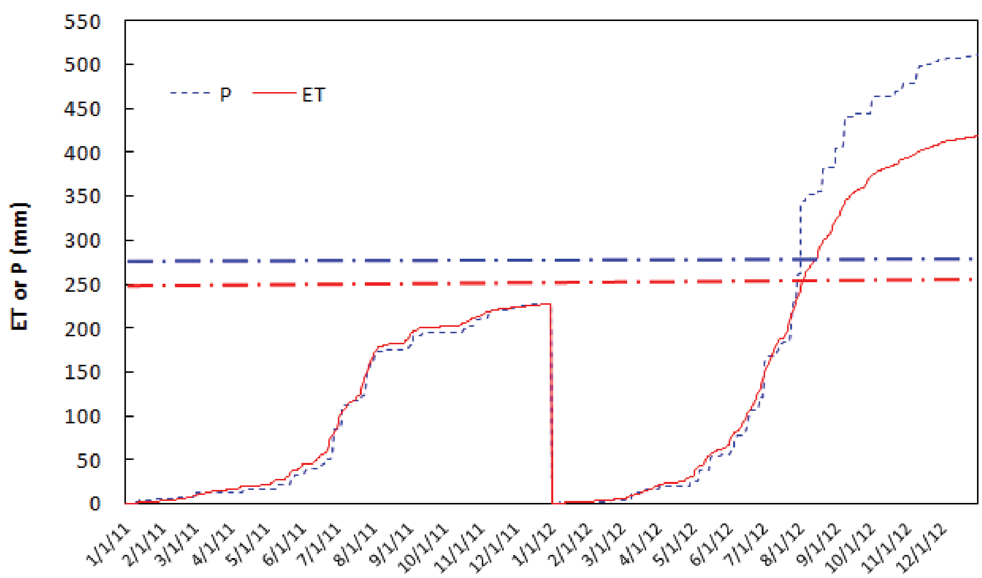

Figure 11. Seasonal contrast of cumulative precipitation (P) and ET in a dry year (2011) and wet year (2012). Dot-dashed lines are long-term mean P (top) and ET (bottom)(1960-2012).

erage precipitation of 275 mm, and consequently the modeled ET was 236 mm year^{-1}, 9 mm higher than the annual precipitation The relative soil moisture in the shallow layers (<50 cm) was lower in the late growing season (August and September) than in April-July due to water use by plants in the growing season. However, the soil moisture differences were small for the deep soil layers (70 cm) (fig. 12b). In the wet year of 2012, the annual precipitation was 512 mm, 237 mm higher than the long-term average precipitation of 275 mm, and the ET was estimated as 415 mm year^{-1}, 161 mm higher than long-term mean of 254 mm year^{-1} (fig. 12c). In this case, the extra rainfall (precipitation – ET = 97 mm, or 19% of precipitation) was available for groundwater recharge. Figure 12c shows that the relative soil moisture in July-September was higher than in April-June in all five soil layers. In contrast, for the extreme dry year of 2005 (fig. 12d), the annual precipitation was only 121 mm, less than half of the long-term mean. Modeled annual ET in 2005 was 151 mm, 30 mm higher than annual precipitation, resulting in a sharp reduction of soil water storage (fig. 12d). In the extreme dry year, relative soil moisture in all five soil layers decreased greatly during July-September, especially in the deep soil layers, suggesting little soil water recharge to deep layers.

ET and Grass Biomass Production

The fresh grass biomass harvested at the end of peak growing season (August) correlated well with modeled peak growing season ET (June-August) (fig. 13a). Similarly, annual mean LAI was also correlated with modeled an-

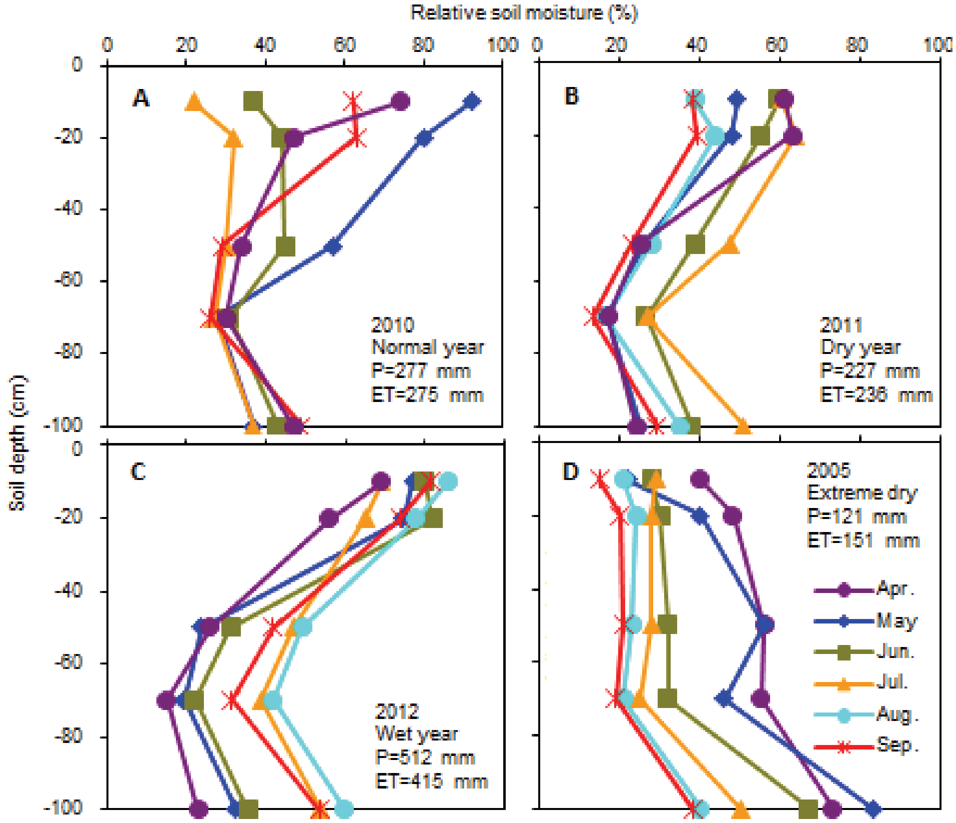

Figure 12. Seasonal relative soil moisture at five soil layers in three typical hydrologic years: (a) 2010 (normal; no data for August), (b) 2011 (dry), (c) 2012 (wet), and (d) 2005 (extreme dry).

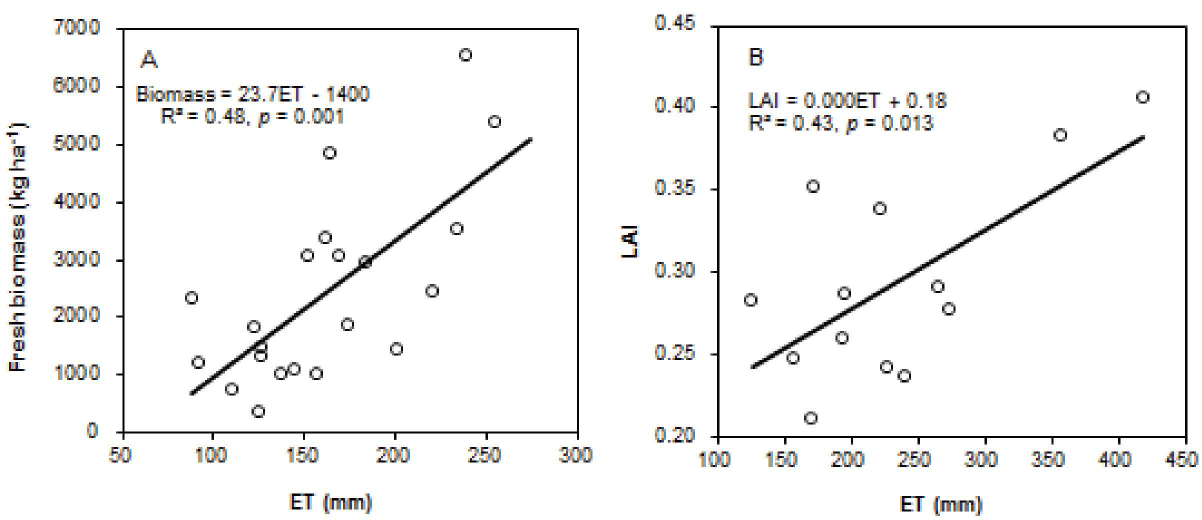

Figure 13. Scatter plots of (a) modeled annual ET during the peak growing season (June-August) with aboveground fresh biomass observed at the end of August (1987-2010), and (b) modeled annual ET with annual mean LAI (2000-2012).

nual ET (fig. 13b). The proportion of ET during the peak growing season to annual ET had a significant decreasing trend (fig. 14) during the past two decades, coincident with the decreasing trend of rainy season precipitation.

Discussion

Dynamics of Soil Moisture in Deep Layers Controlled by Precipitation Pattern and Seasonal Water Balance

Spatial (i.e., horizontal and vertical) and temporal (intra- and inter-annual) variability of soil moisture in the grassland are influenced by a number of environmental and climatic factors, and the effects of these multiple factors are complex because the factors themselves can interact (Zhu et al., 2014). Moisture variation in the upper soil layers following a rainfall event is recognized as an important process in the conversion of rainfall to soil water. It was not surprising that short-term soil moisture content in the shallow layers in this arid environment was tightly controlled by precipitation patterns. However, our long-term monitor-

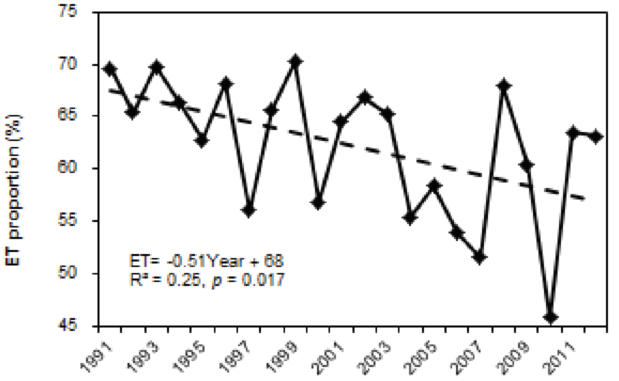

Figure 14. Decreasing trend of the proportion of ET to annual ET during the growing season (June-August) (1991-2012).

ing data show that a drying trend due to lack of precipitation in this grassland ecosystem mostly affected soil moisture in the deep layers (>50 cm). The trends identified at our site were similar to those reported by Li et al. (2010), who simulated soil moisture in Shaanxi Province using the SWAT model for 1951-2004. Their study indicated that the simulated soil moisture at deep depths decreased significantly while shallow layers showed weak decreasing trends, especially for regions with a drier climate. Martínez-Fernández and Ceballos (2003) found that temporal stability of soil moisture is higher in dry conditions than wet conditions. Our soil moisture data in dry versus wet years support this notion (fig. 12). Furthermore, our study suggests that storm size was critical to soil moisture variations in deep layers (70 cm), which received soil water recharge only when the rainfall amount exceeded a certain threshold, approximately 100 mm, depending on antecedent soil moisture conditions. It appears that groundwater recharge occurred only under large storms at the study site.

Since PET greatly exceeded precipitation (fig. 3), and on average over 93% of the annual precipitation was returned to the atmosphere as ET (fig. 10) at the study site, any negative deviation of precipitation from the norm will result in water deficit, and plants will have to use soil water storage to maintain transpiration. ET generally used up or exceeded the growing season precipitation (fig. 11); thus, winter precipitation was important for plant growth in the spring and summer. When dried soil layers form, soil water in the deep layers can be fully replenished only on rare occasions (Liu et al., 2010).

The long-term simulations showed that annual precipitation minus ET, or deep seepage, was negative in half of the years in the recent two decades, which partially explains the decreasing trend of soil moistures in deeper layers. In the recent 20 years, due to a long-term continuous dry and warm climate in the study region, soil moisture replenishment by rainfall during the rainy season was not sufficient to recharge the deep soil moisture storage, leading to a drying trend in deep soils.

Implications of Drying Climate for Grassland Productivity and Groundwater

Soil water resources in deep soil profiles are generally stable due to the insulating effect of the upper soils (Wang et al., 2012). However, in a drying climate, plants may extend their root systems into previously unexplored depths of the soil where water may be available. When soil moisture in the rooting zone (<30 cm for grass) is depleted, the adaptive strategy of the root systems of plants to acquire deep soil water facilitates the increase of actual evapotranspiration and the decrease of deep drainage and groundwater recharge (Eilers et al., 2007). Therefore, continuous droughts in the 2000s at the study site inevitably led to grassland vegetation degradation (fig. 14). Our findings were consistent with the reports by Zhang and Liu (2014) and Wang et al. (2008), which showed that individual extreme drought episodes greatly impacted grassland productivity. However, those simulation studies only examined one severe drought year, and thus it was unclear how a persistent dry climate would contribute to ET and soil moisture dynamics. Our results indicate that persistent droughts can cause prolonged effects on grassland soil hydrology and productivity. Water resources in deep soil profiles thus play an important role in ensuring a well-established vegetation cover. Understanding the impact of climate change on deep soil moisture is essential to quantifying the likely consequences of climate change on grassland ecosystems in the study region.

Future Studies

Soil moisture exhibited high spatial-temporal variability over multiple scales. *In situ* measurements of soil moisture at multiple depths were rather costly in spite of the advances in sensor technologies. For example, advanced microwave sensors can only monitor near-surface soil moisture (0-10 cm) (Eagleman and Lin, 1976; Ma et al., 2001). Satellite microwave sensors have limitations due to their spatial resolution (10 to 50 km) and the uncertainty of complex factors affecting soil surface roughness attenuation (Njoku and Entekhabi, 1996). The best approach to quantifying soil moisture dynamics is coupling *in situ* measurements, remote sensing, and modeling techniques (Li et al., 2010; Zhang and Liu, 2014; Liu et al., 2015).

The physically based MIKE SHE model performed acceptably for modeling daily ET and overall seasonal water balances for two years with little calibration and site-level soil data. This perhaps was not surprising, since ET in an arid climate is mainly controlled by precipitation and daily PET. However, the accuracy of MIKE SHE in simulating soil moisture needs improvement given the low Nash-Sutcliffe model efficiency values (NS < 0.42) achieved. The best approach to quantifying soil moisture dynamics is coupling *in situ* measurements, remote sensing, and modeling techniques. *In situ* soil parameters, including soil moisture release curves for different soil depths, are necessary to fully simulate unsaturated soil water movement (i.e., infiltration and redistribution) and deep seepage. In particular, the soil layer with highly accumulated calcium content that developed in the arid region often impeded soil water infiltration beyond 50 cm, presumably due to low hydraulic conductivity in normal years. In the study region, snowmelt around April often resulted in higher soil moisture, so snow melting processes are important in simulating soil moisture in the spring. Overall, the simulations provide an effective approach to examining the long-term soil moisture dynamics in the entire soil profile.

The regional groundwater table is estimated as about 6 m deep in the study region and has been reported to be in decline due to overuse of water for industrial activities such as mining in Xilinhot. Dried up wetlands are another sign of groundwater overuse in the region. Therefore, we suspect that the drop in the groundwater table may also contribute to the observed decrease in soil moisture in deep soils layers. However, given the modeled positive water balances in the long term, we argue that the main causes of the soil moisture decline were the decrease in precipitation, changes in precipitation characteristics, and increase in soil water deficit.

CONCLUSIONS

Based on long-term *in situ* soil moisture measurements at multiple layers, we found that, over the past two decades, the study site experienced an apparent drying trend, as indicated by the significant decline of soil moisture in the 50-100 cm layer. Long-term simulations with the MIKE SHE model suggested that water balance was negative for half of the time, resulting in a decreasing trend of soil moisture and reduction in grassland ecosystem productivity due to soil water stress. Our study shows that precipitation dominated the water balances that controlled water deficit and seasonal changes of soil moisture. We conclude that the recent persistent drought and reduction of heavy rainfall in the 2000s were the main causes for the decrease of soil moisture in the subsurface soils.

Soil moisture dynamics are important indicators of ecosystem response to global change. The findings from this case study have important implications for assessing the impacts of current and future climate change and human activities on regional water resources and ecosystems. Climate change represents a long-term stressor on grassland ecosystems that have already been affected by increasing resource demands and unsustainable management. Additional research is needed to better model the relative contribution of climate and human influences, such as groundwater withdrawal and grassland grazing, on soil hydrology and grassland productivity under extreme drought events.

ACKNOWLEDGEMENTS

This work was supported by the Natural Science Foundation of China (41571026 and 71373130), the Chinese Meteorological Administration Special Fund for Climate change (CCSF201511), the Chinese Special Fund for Meteorological-Scientific Research in the Public Interest (GYHY201106025), and Jiangsu Key Laboratory of Agricultural Meteorology Fund (KYQ1201). We thank Dr. Jing Xie for sharing soil property data and the China Meteorological Administration for providing meteorological data. Partial support was also from the Southern Research Station, USDA Forest Service.

REFERENCES

Abbott, M. B., Bathurst, J. C., Cunge, J. A., Oconnell, P. E., & Rasmussen, J. (1986a). An introduction to the European Hydrological System - Systeme Hydrologique Europeen (SHE): 1. History and philosophy of a physically based, distributed modeling system. *J. Hydrol., 87*(1-2), 45-59. http://dx.doi.org/10.1016/0022-1694(86)90114-9

Abbott, M. B., Bathurst, J. C., Cunge, J. A., Oconnell, P. E., & Rasmussen, J. (1986b). An Introduction to the European Hydrological System - Systeme Hydrologique Europeen (SHE): 2. Structure of a physically based, distributed modeling system. *J. Hydrol., 87*(1-2), 61-77. http://dx.doi.org/10.1016/0022-1694(86)90115-0.

Allen, R. G., Pereira, L. S., Raes, D., & Smith, M. (1998). Crop evapotranspiration: Guidelines for computing crop water requirements. FAO Irrigation and Drainage Paper No. 56. Rome, Italy: United Nations FAO.

Brocca, L., Morbidelli, R., Melone, F., & Moramarco, T. (2007). Soil moisture spatial variability in experimental areas of central Italy. *J. Hydrol., 333*(2-4), 356-373. http://dx.doi.org/10.1016/j.jhydrol.2006.09.004.

Brubaker, K. L., & Entekhabi, D. (1996). Analysis of feedback mechanisms in land-atmosphere interaction. *Water Resour. Res., 32*(5), 1343-1357. http://dx.doi.org/10.1029/96WR00005.

Chanasyk, D. S., Mapfumo, E., & Willms, W. (2003). Quantification and simulation of surface runoff from fescue grassland watershed. *Agric. Water Mgmt., 59*(2), 137-153. http://dx.doi.org/10.1016/S0378-3774(02)00124-5.

Dai, Z., Li, C., Trettin, C., Sun, G., Amatya, D., & Li, H. (2010). Bi-criteria evaluation of the MIKE SHE model for a forested watershed on the South Carolina coastal plain. *Hydrol. Earth Syst. Sci., 14*(6), 1033-1046. http://dx.doi.org/10.5194/hess-14-1033-2010.

DHI. (2004). MIKE SHE: An integrated hydrological modeling system. Copenhagen, Denmark: Danish Hydraulic Institute.

Eagleman, J. R., & Lin, W. C. (1976). Remote sensing of soil moisture by a 21-cm passive radiometer. *J. Geophys. Res., 81*(21), 3660-3666. http://dx.doi.org/10.1029/JC081i021p03660.

Eilers, V. H. M., Carter, R. C., & Rushton, K. R. (2007). A single-layer soil water balance model for estimating deep drainage (potential recharge): An application to cropped land in semi-arid northeast Nigeria. *Geoderma, 140*(1-2), 119-131. http://dx.doi.org/10.1016/j.geoderma.2007.03.011.

Famiglietti, J. S., Rudnicki, J. W., & Rodell, M. (1998). Variability in surface moisture content along a hillslope transect: Rattlesnake Hill, Texas. *J. Hydrol., 210*(1-4), 259-281. http://dx.doi.org/10.1016/S0022-1694(98)00187-5.

Fay, P. A., Carlisle, J. D., Knapp, A. K., Blair, J. M., & Collins, S. L. (2003). Productivity responses to altered rainfall patterns in a C-4-dominated grassland. *Oecologia, 137*(2), 245-251. http://dx.doi.org/10.1007/s00442-003-1331-3.

Grassini, P., You, J. S., Hubbard, K. G., & Cassman, K. G. (2010). Soil water recharge in a semi-arid temperate climate of the central U.S. Great Plains. *Agric. Water Mgmt., 97*(7), 1063-1069. http://dx.doi.org/10.1016/j.agwat.2010.02.019.

Han, E. J., Merwade, V., & Heathman, G. C. (2012). Implementation of surface soil moisture data assimilation with watershed scale distributed hydrological model. *J. Hydrol., 416-417*, 98-117. http://dx.doi.org/10.1016/j.jhydrol.2011.11.039.

Hao, L., Sun, G., Liu, Y. Q., Gao, Z. Q., He, J. J., Shi, T. T., & Wu, B. J. (2014). Effects of precipitation on grassland ecosystem restoration under grazing exclusion in Inner Mongolia, China. *Landscape Ecol., 29*(10), 1657-1673. http://dx.doi.org/10.1007/s10980-014-0092-1.

Hao, L., Sun, G., Liu, Y. Q., & Qian, H. (2015). Integrated modeling of water supply and demand under management

options and climate change scenarios in Chifeng City, China. *JAWRA, 51*(3), 655-671. http://dx.doi.org/10.1111/1752-1688.12311.
Heathman, G. C., Cosh, M. H., Merwade, V., & Han, E. J. (2012). Multi-scale temporal stability analysis of surface and subsurface soil moisture within the Upper Cedar Creek watershed, Indiana. *Catena, 95*, 91-103. http://dx.doi.org/10.1016/j.catena.2012.03.008.
Jia, Y. H., & Shao, M. A. (2014). Dynamics of deep soil moisture in response to vegetational restoration on the Loess Plateau of China. *J. Hydrol., 519*(A), 523-531. http://dx.doi.org/10.1016/j.jhydrol.2014.07.043.
Joshi, C., Mohanty, B. P., Jacobs, J. M., & Ines, A. V. M. (2011). Spatiotemporal analyses of soil moisture from point to footprint scale in two different hydroclimatic regions. *Water Resour. Res., 47*(1), W01508. http://dx.doi.org/10.1029/2009WR009002.
Kendall, M. G. (1975). *Rank Correlation Methods.* London, U.K.: Charles Griffin.
Kristensen, K. J., & Jensen, S. E. (1975). A model for estimating actual evapotranspiration from potential evapotranspiration. *Nordic Hydrol., 6*(3), 170-188.
Li, M. X., Ma, Z. G., & Du, J. W. (2010). Regional soil moisture simulation for Shaanxi Province using SWAT model validation and trend analysis. *Sci. China Earth Sci., 53*(4), 575-590. http://dx.doi.org/10.1007/s11430-010-0031-1.
Li, M. X., Ma, Z. G., & Niu, G. Y. (2011). Modeling spatial and temporal variations in soil moisture in China. *Chinese Sci. Bull., 56*(17), 1809-1820. http://dx.doi.org/10.1007/s11434-011-4493-0.
Liu, W., Zhang, X. C., Dang, T. H., Zhu, O. Y., Li, Z., Wang, J., Wang, R., & Gao, C. Q. (2010). Soil water dynamics and deep soil recharge in a record wet year in the southern Loess Plateau of China. *Agric. Water Mgmt., 97*(8), 1133-1138. http://dx.doi.org/10.1016/j.agwat.2010.01.001.
Liu, Y. L., Zhuang, Q. L., Chen, M., Pan, Z. H., Tchebakova, N., Sokolov, A., Kicklighter, D., Melillo, J., Sirin, A., Zhou, G. S., He, Y. J., Chen, J. Q., Bowling, L., Miralles, D., & Parfenova, E. (2013). Response of evapotranspiration and water availability to changing climate and land cover on the Mongolian Plateau during the 21st century. *Global Planet. Change, 108*, 85-99. http://dx.doi.org/10.1016/j.gloplacha.2013.06.008.
Liu, C., Sun, G., McNulty, S. G., & Kang, S. (2015). An improved evapotranspiration model for an apple orchard in northwestern China. *Trans ASABE, 58*(5), 1253-1264.
Lu, J. B., Sun, G., McNulty, S. G., & Comerford, N. B. (2009). Sensitivity of pine flatwoods hydrology to climate change and forest management in Florida, U.S. *Wetlands, 29*(3), 826-836. http://dx.doi.org/10.1672/07-162.1
Ma, Z. G., Fu, C. B., Xie, L., Chen, W. H., & Tao, S. W. (2001). Some problems in the study on the relationship between soil moisture and climatic change. *Adv. Earth Sci., 16*(4), 563-568.
Mann, H. B. (1945). Non-parametric test against trend. *Econometrica, 13*(3), 245-259. http://dx.doi.org/10.2307/1907187.
Martínez-Fernández, J., & Ceballos, A. (2003). Temporal stability of soil moisture in a large-field experiment in Spain. *SSSA J., 67*(6), 1647-1656. http://dx.doi.org/10.2136/sssaj2003.1647.
McMichael, C. E., Hope, A. S., & Loaiciga, H. A. (2006). Distributed hydrological modelling in California semi-arid shrublands: MIKE SHE model calibration and uncertainty estimation. *J. Hydrol., 317*(3-4), 307-324. http://dx.doi.org/10.1016/j.jhydrol.2005.05.023.
Mohanty, B. P., Shouse, P. J., & van Genuchten, M. Th. (1998). Spatio-temporal dynamics of water and heat in a field soil. *Soil Tillage Res., 47*(1-2), 133-143. http://dx.doi.org/10.1016/S0167-1987(98)00084-1.
Njoku, E. G., & Entekhabi, D. (1996). Passive microwave remote sensing of soil moisture. *J. Hydrol., 184*(1-2), 101-129. http://dx.doi.org/10.1016/0022-1694(95)02970-2.
Qi, J. G., Chen, J. Q., Wan, S. Q., & Ai, L. K. (2012). Understanding the coupled natural and human systems in dryland East Asia. *Environ. Res. Letters, 7*(1), 015202. http://dx.doi.org/10.1088/1748-9326/7/1/015202.
Ritter, A., & & Muñoz-Carpena, R. (2013). Predictive ability of hydrological models: Objective assessment of goodness-of-fit with statistical significance. *J. Hydrol., 480*(1), 33-45. http://dx.doi.org/10.1016/j.jhydrol.2012.12.004.
Robock, A.,Vinnikov, K. Y., Srinivasan, G., Entin, J. K., Hollinger, S. E., Speranskaya, N. A., Liu, S., & Namkhal, A. (2000). The global soil moisture data bank. *Bull. American Meteorol. Soc., 81*(6), 1281-1299.
Sala, O. E., Lauenroth, W. K., & Parton, W. J. (1992). Long-term soil water dynamics in the shortgrass steppe. *Ecology, 73*(4), 1175-1181. http://dx.doi.org/10.2307/1940667.
Shao, C. L., Chen, J. Q., & Li, L. H. (2013). Grazing alters the biophysical regulation of carbon fluxes in a desert steppe. *Environ. Res. Letters, 8*(2), 025012. http://dx.doi.org/10.1088/1748-9326/8/2/025012.
Starks, P. J., Heathman, G. C., Ahuja, L. R., & Ma, L. W. (2003). Use of limited soil property data and modeling to estimate root zone soil water content. *J. Hydrol., 272*(1-4), 131-147. http://dx.doi.org/10.1016/S0022-1694(02)00260-3.
Sun, G., McNulty, S. G., Lu, J., Amatya, D. M., Liang, Y., & Kolka, R. K. (2005). Regional annual water yield from forest lands and its response to potential deforestation across the southeastern U.S. *J. Hydrol., 308*(1-4), 258-268. http://dx.doi.org/10.1016/j.jhydrol.2004.11.021.
Sun, G., Lu, J., McNulty, S. G., Vose, J. M., & Amayta, D. M. (2006). Using the hydrologic model MIKE SHE to assess disturbance impacts on watershed processes and responses across the southeastern U.S. *Proc. 2nd Interagency Conf. on Research in the Watersheds* (pp. 41-53). Otto, N.C.: USDA Forest Service, Coweeta Hydrologic Laboratory.
Sun, G., Zuo, C. Q., Liu, S. Y., Liu, M. L., McNulty, S. G., & Vose, J. M. (2008). Watershed evapotranspiration increased due to changes in vegetation composition and structure under a subtropical climate. *JAWRA, 44*(5), 1164-1175. http://dx.doi.org/10.1111/j.1752-1688.2008.00241.x.
Tague, C., McMichael, C., Hope, A., Choate, J., & Clark, R. (2004). Application of the RHESSys model to a California semi-arid shrubland watershed. *JAWRA, 40*(3), 575-589. http://dx.doi.org/10.1111/j.1752-1688.2004.tb04444.x.
Tombul, M. (2007). Mapping field surface soil moisture for hydrological modeling. *Water Resour. Mgmt., 21*(11), 1865-1880. http://dx.doi.org/10.1007/s11269-006-9134-z.
van Genuchten, M. T., Simunek, J., Leij, F. J., & Sejna, M. (1998). RETC, Version 6.0: Code for quantifying the hydraulic functions of unsaturated soils. Riverside, Cal.: USDA-ARS Salinity Laboratory.
Wang, Y. F., Mo, X. G., Hao, Y. B., Guo, R. P., Huang, X. Z., & Wang, Y. F. (2008). Simulating seasonal and interannual variations of ecosystem evapotranspiration and its components in Inner Mongolia steppe with VIP model. *J. Plant Ecol., 32*(5), 1052-1060.
Wang, Y. Q., Shao, M. A., Liu, Z. P., & Warrington, D. N. (2012). Regional spatial pattern of deep soil water content and its influencing factors. *Hydrol. Sci. J., 57*(2), 265-281. http://dx.doi.org/10.1080/02626667.2011.644243.
Wang, Y. Q., Shao, M. A., Liu, Z. P., & Horton, R. (2013). Regional-scale variation and distribution patterns of soil saturated hydraulic conductivities in surface and subsurface layers in the loessial soils of China. *J. Hydrol., 487*, 13-23. http://dx.doi.org/10.1016/j.jhydrol.2013.02.006.

Wendroth, O., Pohl, W., Koszinski, S., Rogasik, H., Ritsema, C. J., & Nielsen, D. R. (1999). Spatio-temporal patterns and covariance structures of soil water status in two northeast German field sites. *J. Hydrol., 215*(1-4), 38-58. http://dx.doi.org/10.1016/S0022-1694(98)00260-1.

Xie, J., Guan, W. B., Cui, G. F., Sun, G., Chen, J. Q., Wang, M., & Qi, Z. D. (2009). Soil moisture characteristics of different types of vegetation in Xilingol grassland [in Chinese with English abstract]. *J. Northeast Forestry Univ., 37*(1), 45-48.

Yang, L., Chen, L., & Wei., W. (2014). Effects of vegetation restoration on the spatial distribution of soil moisture at the hillslope scale in semi-arid regions. *Catena, 124*, 138-146. http://dx.doi.org/10.1016/j.catena.2014.09.014.

Zhang, N., & Liu, C. Y. (2014). Simulated water fluxes during the growing season in semi-arid grassland ecosystems under severe drought conditions. *J. Hydrol., 512*, 69-86. http://dx.doi.org/10.1016/j.jhydrol.2014.02.056.

Zhang, P. P., & Shao, M. A. (2013). Temporal stability of surface soil moisture in a desert area of northwestern China. *J. Hydrol., 505*, 91-101. http://dx.doi.org/10.1016/j.jhydrol.2013.08.045.

Zhang, Z. Q., Wang, S. P., Sun, G., McNulty, S. G., Zhang, H. Y., Li, J. L., Zhang, M. L., Klaghofer, E., & Strauss, P. (2008). Evaluation of the MIKESHE model for application in the Loess Plateau, China. *JAWRA*, *44*(5), 1108-1120. http://dx.doi.org/10.1111/j.1752-1688.2008.00244.x.

Zhou, G., & Wang, Y. (2002). Response of grassland plant community along northeast China transect to water gradient. *J. Veg. Sci., 13*(3), 361-368. http://dx.doi.org/10.1111/j.1654-1103.2002.tb02060.x.

Zhu, H. D., Shi, Z. H., Fang, N. F., Wu, G. L., Guo, Z. L., & Zhang, Y. (2014). Soil moisture response to environmental factors following precipitation events in a small catchment. *Catena, 120*, 73-80. http://dx.doi.org/10.1016/j.catena.2014.04.003.